

## Adsorption efficiency of electrospun polyacrylonitrile nanofibers modified with ethylenediamine for nitrate removal

Choon-Ki Na<sup>a</sup>, Gayeon Park<sup>a</sup>, Han Yong Kim<sup>b</sup>, Hyunju Park<sup>c,\*</sup>

<sup>a</sup>Department of Environmental Engineering, Mokpo National University, Jeonnam 58554, South Korea, emails: nack@mokpo.ac.kr (C.-K. Na), cdefghijk246@naver.com (G. Park)

<sup>b</sup>School of Environmental Engineering, University of Seoul, Seoul 02504, South Korea, email: kimhy@taeyoung.com

<sup>c</sup>Institute of Engineering Research, Seoul National University, Seoul 08826, South Korea, email: narjjis@snu.ac.kr

Received 20 August 2023; Accepted 3 December 2023

### ABSTRACT

This study investigates the potential of electrospun polyacrylonitrile (PAN) nanofibers chemically modified with ethylenediamine (EDA) as effective adsorbents for nitrate–nitrogen (NO<sub>3</sub>–N) removal from wastewater. The nanofibers treated with 100% EDA at 95°C exhibited the highest adsorption capacity of 47 mg/g at 5 h of reaction time, whereas those at 80°C showed an increased adsorption capacity over time, reaching 46 mg/g after 15 h. Optimal NO<sub>3</sub>–N adsorption was observed in the weakly acidic pH range (3–6). This study also explored the field applicability and regeneration potential of PAN-EDA nanofibers. An adsorption–regeneration experiment involving fixed-bed columns showed promising results, with the adsorbent's performance sustained over multiple uses. Overall, this study concluded that PAN-EDA nanofibers are effective and reusable adsorbents for nitrate removal, paving the way for more sustainable wastewater treatment strategies.

**Keywords:** Adsorption; Ethylenediamine modification; Nitrate removal; Polyacrylonitrile; Wastewater treatment

### 1. Introduction

Nitrate–nitrogen contamination is recognized as a significant environmental and health concern, originating from diverse sources such as sewage, agricultural runoff, and industrial discharges [1]. Nitrate salts, nitrate ions, and common nitrogen compounds contribute to water pollution, eutrophication, and potential adverse health effects [2]. Nitrate–nitrogen, when present in elevated concentrations in drinking water, poses a significant threat to human health, potentially causing methemoglobinemia (“blue baby syndrome”) and even cancer. Traditional approaches for mitigating nitrate contamination encounter limitations, including high costs, reduced removal efficiency and the generation of undesirable byproducts [3]. Consequently, alternative strategies for developing effective and sustainable nitrate–nitrogen removal technologies are imperative.

Chemical treatment methods for nitrate–nitrogen removal include photocatalytic decomposition, electrochemical processes, membrane separation, and adsorption [4,5]. While photocatalytic and electrochemical methods offer the advantages of relatively straightforward process management and maintenance, they are associated with high chemical and energy consumption.

Adsorption processes, contrastingly, offer distinct advantages, as they selectively remove ionized substances such as nitrate and ions of heavy metals without the risk of secondary pollutant generation, ensuring consistent treatment efficiency. Consequently, adsorption processes represent versatile and cost-effective unit operations that can be easily integrated into advanced treatment systems. Extensive efforts have been devoted to the development of adsorbent materials endowed with multifunctionality, high efficiency, selectivity, and economic viability.

\* Corresponding author.

In recent times, there has been a growing trend in the field of environmental remediation, focusing on the promising application of polyacrylonitrile (PAN) fibers as nitrate adsorbents, owing to their unique physicochemical properties [6–8]. PAN fibers are characterized by high thermal stability, excellent mechanical strength, and the ability to be readily functionalized with abundant amino groups, enhancing their adsorption capacity [9]. In recent years, considerable research has been directed toward improving the nitrate–nitrogen adsorption performance of PAN fibers. Surface modification techniques such as plasma treatment, chemical grafting, and heat treatment have been employed to increase the surface roughness and porosity of PAN fibers, thus enhancing their adsorption capabilities [10]. However, despite these promising trends, the development of nitrate adsorbents based on PAN remains challenging. One of the key concerns is the optimization of fiber morphology to achieve maximum adsorption. Fine fibers offer a larger surface area for adsorption but tend to form dense networks that restrict the accessibility of adsorbate molecules to the fiber surface [11,12].

Recently, electrospinning, a technique involving an electric field to produce fine fibers, has been actively explored in various fields. Jasna et al. [13] employed electrostatic self-assembly to create cellulose nanofibers and for the development of stable and efficient functional materials for seawater evaporation and purification. Yang et al. [14] immobilized laccase on a composite hydrogel of functionalized cellulose nanofibers and alginate, effectively degrading bisphenol A in polluted water.

This study places particular emphasis on the development of innovative adsorbents for nitrate–nitrogen removal by modifying PAN nanofibers using electrospinning. Electrospinning enables the production of PAN nanofibers with high surface area and porosity. To enhance these features, ethylenediamine (EDA) was introduced as a modifier to create PAN-EDA nanofibers. This research systematically investigates the chemical modification process of nanofibers and characterizes the resulting materials. The primary objective of this study is to examine the structural changes and adsorption performance of PAN-EDA nanofibers to contribute to the development of an effective and sustainable adsorbent for nitrate–nitrogen removal. The insights gained from this research highlight the potential of modified nanofibers as a novel approach to address nitrate contamination and provide valuable insights into potential applications, thereby advancing the fields of water treatment and environmental remediation.

## 2. Materials and methods

### 2.1. Preparation of adsorbent

Electrospun PAN nanofibers were used as substrate polymer fibers to synthesize nitrate–nitrogen adsorbents. EDA ( $\geq 99\%$ , Sigma-Aldrich, USA) was purchased from the manufacturer and used as the monomer for the amination reaction without purification.

The electrospun PAN nanofibers were modified as follows: approximately 0.2 g of the PAN fibers was refluxed with EDA in an oil bath at a temperature of 80°C–95°C for

2–15 h. The resulting aminated nanofibers (PAN-EDA) were washed with deionized water and dried in an oven at 60°C until a constant weight was achieved. Upon completion of the reaction, the nanomaterial was neutralized with a 2-M HCl solution, extensively rinsed with deionized water, and then dried in an oven at 50°C. The modified nanofibers were stored in a desiccator for further use.

### 2.2. Adsorption experiment and analysis

A batch adsorption experiment was conducted using artificial wastewater to evaluate the adsorption performance of PAN-EDA nanofibers. The batch adsorption experiment involved adding 0.1 g of the adsorbent to 100 mL of the adsorbate solution and stirring the mixture at 120 rpm at 25°C for 24 h, utilizing a rotary constant temperature stirrer. The residual anion concentration after adsorption was analyzed using UV-Vis spectrophotometry (Shimadzu UV-2401PC, Japan) according to the standardized water quality process test method. The adsorption capacity (mg/g) was calculated based on the difference in the anion mass between the filtrate before and after adsorption:

$$q = \frac{V(C_0 - C_e)}{W}$$

where  $q$  represents the adsorption capacity (mg/g) per gram of adsorbent at equilibrium;  $C_0$  and  $C_e$  are the initial and equilibrium concentrations of the adsorbate in the solution, respectively;  $V$  is the volume of the solution (L); and  $W$  is the mass of the adsorbent added (g). Additionally, a fixed-bed column adsorption experiment was conducted in continuous flow mode at room temperature using a polyethylene column with an inner diameter of 4.6 mm. The fixed-bed column was filled with PAN-EDA nanofibers, controlling a height-to-diameter ratio of 0.28 and a packing density of 0.46. To assess the regeneration efficiency of the adsorbent, desorption of the adsorbate was achieved using a 1.0-M NaCl and HCl solution, followed by rinsing with distilled water after each cycle of the fixed-bed column adsorption experiments.

Scanning electron microscopy (SEM) was used to observe changes in the surface morphology of the PAN and PAN-EDA nanofibers. The chemical structures of the PAN and PAN-EDA nanofibers were analyzed using Fourier-transform infrared (FTIR) spectroscopy using an infrared spectrophotometer (Shimadzu IR-435, Japan).

## 3. Results and discussion

### 3.1. Adsorbent preparation

To find the optimum reaction conditions for the amination of PAN nanofiber, the effects of the reaction time and temperature, and the concentration of EDA on the amination of PAN nanofiber were investigated. The degree of amination was confirmed by the nitrate–nitrogen ( $\text{NO}_3\text{-N}$ ) adsorption capacity of the resulting aminated PAN products. Fig. 1 shows the effect of reaction time on the amination of PAN nanofibers and its impact on the adsorption capacities of the resulting aminated PAN-EDA nanofibers. All reactions were

conducted at 95°C with 100% EDA. As shown in Fig. 1, the  $\text{NO}_3^-$ -N adsorption capacity increased with the extension of the reaction time up to 5 h and then slightly decreased.

Fig. 2 shows the influence of reaction temperature for the amination of PAN nanofiber on the adsorption capacities of the resulting PAN-EDA nanofibers. All reactions were conducted at 80°C and 95°C for durations ranging from 5 to 15 h, with 100% EDA. As shown in Fig. 2, the PAN-EDA nanofiber aminated at 95°C exhibited a maximum adsorption capacity of 47 mg/g at a reaction time of 5 h, with a subsequent decrease as the reaction time increased. Conversely, the PAN-EDA nanofiber aminated at 80°C demonstrated an initial adsorption capacity of 26 mg/g after 5 h, which increased with prolonged reaction time, reaching 46 mg/g after 15 h. The variations in adsorption tendencies depending on the amination reaction temperature can be attributed to the impact of temperature on the surface properties and functional groups of the PAN-EDA nanofibers. Higher

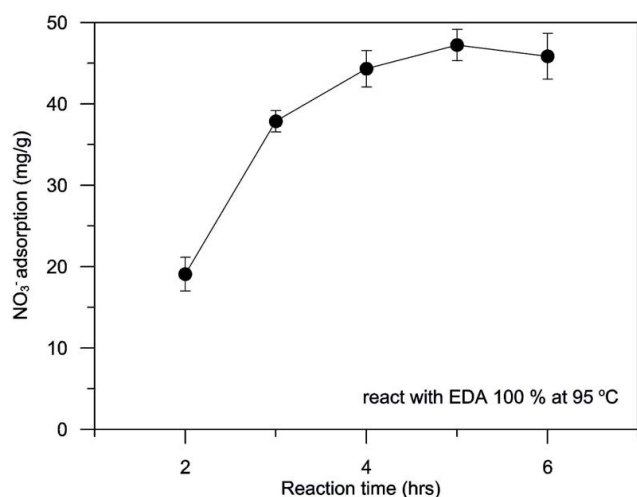


Fig. 1. Effect of reaction time on the amination of polyacrylonitrile nanofiber.

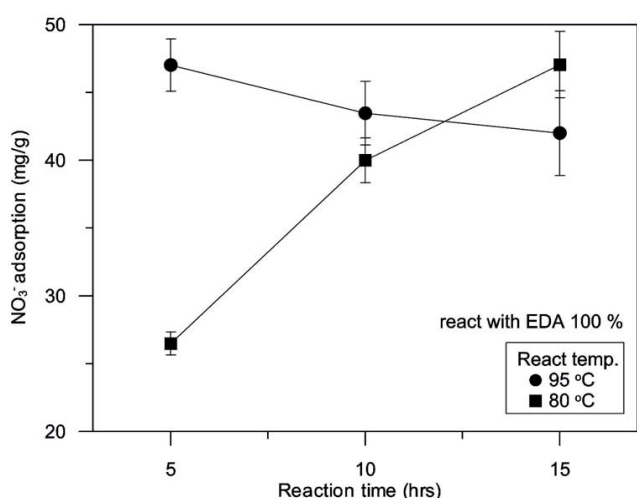


Fig. 2. Effect of reaction temperature on the amination of polyacrylonitrile nanofiber.

amination reaction temperatures (95°C in this case) likely facilitated a higher degree of functionalization, resulting in more active adsorption sites for nitrate ions [11]. However, as the reaction progresses, higher temperatures may also contribute to the degradation or alteration of adsorption sites, leading to a decrease in overall adsorption capacity over time [15].

Fig. 3 shows the impact of EDA concentration on the adsorption capacities of aminated PAN-EDA nanofibers. All reactions were carried out at 95°C for 5 h with 33%, 50%, and 100% EDA. As shown in Fig. 3, the  $\text{NO}_3^-$ -N adsorption capacity of the PAN-EDA nanofiber aminated with 100% EDA was highest (48 mg/g) at 5 h and then decreased with increasing reaction time, whereas those of the PAN-EDA nanofibers aminated using 33% and 50% EDA increased until 10 h and then levelled-off. After a reaction time of more than 10 h, the PAN-EDA nanofiber aminated with 50% EDA exhibited a higher adsorption capacity than the case using 100% EDA.

This observed pattern can be ascribed to the complex interplay among EDA concentration, surface functionalization, and reaction kinetics. When EDA concentration is higher, a larger quantity of amino groups becomes accessible for engaging with nitrate ions, which results in elevated initial adsorption rates. Nevertheless, as the reaction advances, surface saturation takes place, restricting the availability of unoccupied amino groups. Consequently, this leads to a gradual decline in adsorption capacity over time. The presence of a 50% EDA concentration appears to establish an equilibrium between having an adequate number of amino groups for adsorption and maintaining sustained adsorption capacity.

### 3.2. Physico-chemical properties of the adsorbent

The physico-chemical properties of the adsorbent were investigated by focusing on the structural changes induced by the chemical modification of the PAN nanofibers. SEM analysis was conducted to examine the surface morphologies of the PAN and PAN-EDA nanofibers. SEM images are

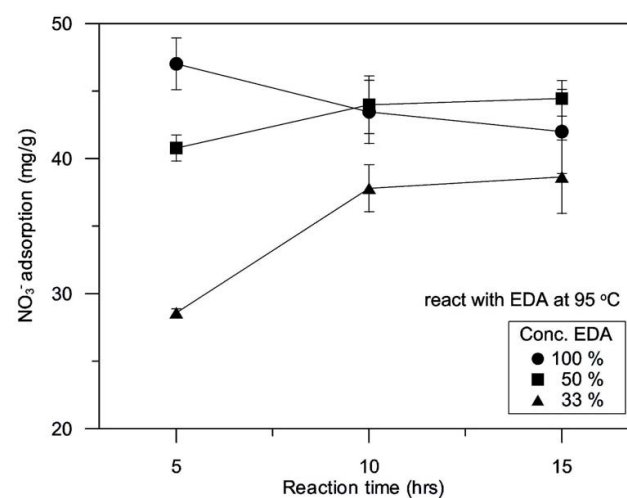


Fig. 3. Effect of ethylenediamine concentration on the amination of polyacrylonitrile nanofiber.

shown in Fig. 4. show that the PAN and PAN-EDA nanofibers have similar average diameters of approximately  $289 \pm 31$  nm and  $288 \pm 68$  nm, respectively. Chemical modification using EDA resulted in negligible changes in the average diameter of the nanofibers, although some variations in size were observed [16].

FTIR spectroscopy was performed to analyze the chemical groups present in the PAN and PAN-EDA nanofibers. The infrared spectra in Fig. 5 reveal the characteristic absorption frequencies of the various functional groups. The absorption peaks observed in the PAN nanofibers were assigned as follows:  $3,437\text{ cm}^{-1}$  for OH stretching,  $2,939$  and  $2,872\text{ cm}^{-1}$  for CH stretching in  $\text{CH}$ ,  $\text{CH}_2$ , and  $\text{CH}_3$  groups,  $2,243\text{ cm}^{-1}$  for  $\text{C}\equiv\text{N}$  stretching,  $1,734\text{ cm}^{-1}$  for  $\text{C}=\text{O}$  stretching,  $1,454\text{ cm}^{-1}$  for CH bending,  $1,384\text{ cm}^{-1}$  for symmetric blending of  $\text{CH}_3$  in  $\text{CCH}_3$ , and  $1,072\text{ cm}^{-1}$  for  $\text{C}-\text{O}$  stretching in acetate ester.

After chemically modifying PAN with EDA, significant changes were observed in the FTIR spectra of the resulting PAN-EDA nanofibers. The weak and broad peak at  $3,437\text{ cm}^{-1}$ , attributed to OH stretching in PAN nanofibers, transformed into a strong and broadband with a maximum frequency at  $3,389\text{ cm}^{-1}$  in PAN-EDA nanofibers. This band resulted from the combined intensities of the OH and NH stretching and vibration bands on the surface of the PAN-EDA nanofibers, as reported in previous studies involving the chemical binding of diethylenetriamine with PAN fibers [17]. The intensity reduction of the peak at  $2,243\text{ cm}^{-1}$  in the PAN-EDA nanofibers indicates the partial conversion of surface nitrile groups to amidine groups ( $\text{N}-\text{C}=\text{N}$ ) during the formation process, as supported by the absorption at wavenumber  $1,639\text{ cm}^{-1}$  [18].

Furthermore, reductions in the peak intensities at  $1,731\text{ cm}^{-1}$  ( $\text{C}=\text{O}$  stretching),  $1,454\text{ cm}^{-1}$  (CH bending),  $1,384\text{ cm}^{-1}$  (symmetric blending of  $\text{CH}_3$  in  $\text{CCH}_3$ ), and  $1,072\text{ cm}^{-1}$  ( $\text{C}-\text{O}$  stretching) suggested the hydrolysis of esters of itaconic and methacrylic acid monomers [17]. New peaks appeared at  $1,674$  and  $1,612\text{ cm}^{-1}$ , assigned to the stretching vibrations of the  $\text{C}=\text{O}$  groups in amides and primary amines ( $\text{NH}_2$ ), respectively.

### 3.3. Adsorption properties

The effect of pH on the adsorption capacity of the PAN-EDA nanofibers for  $\text{NO}_3^-$ -N was explored by preparing a pH 2–10 solution containing  $1\text{ mM NO}_3^-$ -N, with pH

adjustments made using  $1.0\text{ N HCl}$  and  $\text{NaOH}$ . Adsorption tests were conducted by adding  $0.5\text{ g}$  of the adsorbent to  $1\text{ L}$  of wastewater. Fig. 6 shows the recorded pH values of

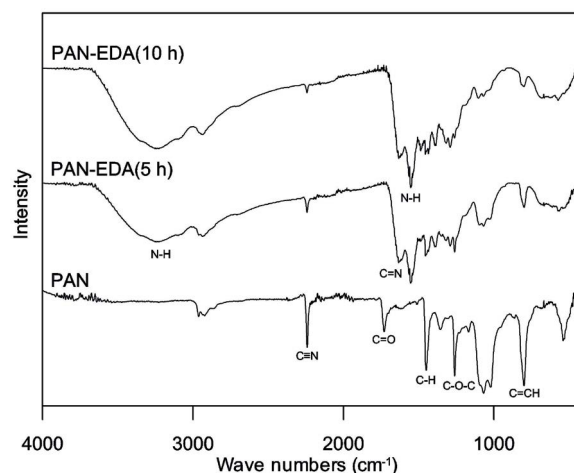


Fig. 5. Fourier-transform infrared spectra of polyacrylonitrile, polyacrylonitrile-ethylenediamine (5 h), and polyacrylonitrile-ethylenediamine (10 h) nanofibers.

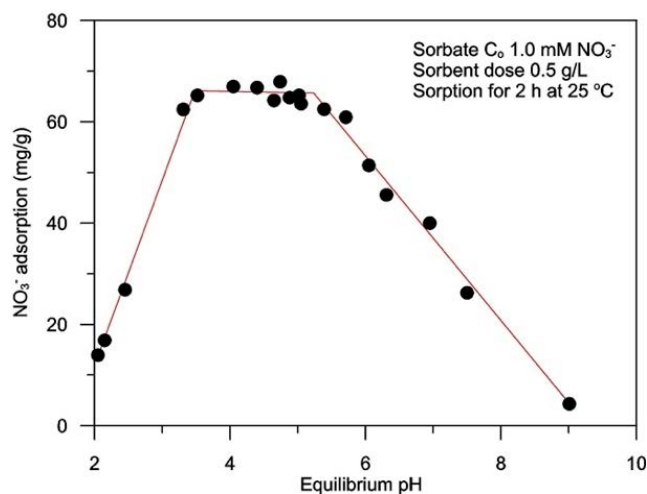


Fig. 6. Comparison of  $\text{NO}_3^-$ -N adsorption capacity according to pH change.

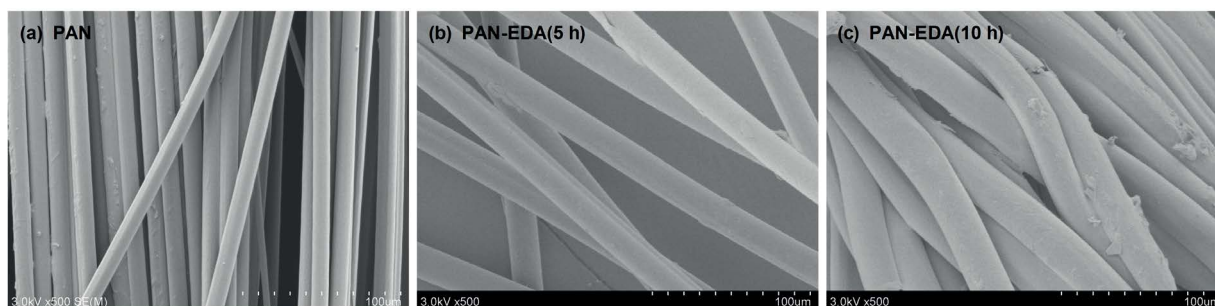


Fig. 4. Scanning electron microscopy images of polyacrylonitrile (a), polyacrylonitrile-ethylenediamine (5 h) (b), and polyacrylonitrile-ethylenediamine (10 h) nanofibers (c).

the solution and the corresponding adsorption quantities of the  $\text{NO}_3^-$ -N post-adsorption reaction [9].

The  $\text{NO}_3^-$ -N adsorption rate by the PAN-EDA nanofiber adsorbent was the highest (68 mg/g) within the weakly acidic pH range (pH 3–6). As the pH increased towards the alkaline region,  $\text{NO}_3^-$ -N adsorption capacity declined, with limited adsorption observed beyond pH 9 [16]. The variation in  $\text{NO}_3^-$ -N adsorption capacity with the pH alteration can be attributed to factors such as adsorbent surface degradation and  $\text{NO}_3^-$ -N species differentiation [19].

The pH of the solution affects the surface charge of the PAN-EDA nanofiber adsorbent. At low pH (acidic conditions), the solution becomes positively charged, which promotes electrostatic interactions between the positively charged surface of the nanofiber and the negatively charged  $\text{NO}_3^-$ -N ions, thereby increasing the adsorption capacity. The surface charge in the weakly acidic range (pH 3–6) is optimal for strong electrostatic attraction and improved adsorption of  $\text{NO}_3^-$ -N [16].

Additionally, pH changes can affect  $\text{NO}_3^-$ -N differentiation in the solution. At low pH values,  $\text{NO}_3^-$ -N can be present as non-separated nitric acid ( $\text{HNO}_3$ ) or protonated nitric acid ions ( $\text{NO}_3^-$ ). These species are more easily adsorbed by the PAN-EDA nanofiber adsorbents because of their strong electrostatic interactions. As the pH increases to alkaline conditions,  $\text{NO}_3^-$ -N is mainly present as dissociated nitrate ions ( $\text{NO}_3^-$ ), which can lead to weak electrostatic interactions with the nanofiber surfaces, thus reducing the adsorption capacity [20].

To assess the field applicability and regeneration potential of the PAN-EDA nanofiber adsorbent, its adsorption and regeneration capabilities were evaluated using fixed-bed columns. In the adsorption–constriction experiment, artificial wastewater containing 62 mg/L of  $\text{NO}_3^-$ -N ions was injected into a fixed-bed column ( $H/D = 2.83$ ) at a flow rate of 0.15 cm/s. The adsorption–regeneration experiment involved injecting the regeneration solution at the same flow rate as the adsorption process and rinsing with distilled water until the effluent  $\text{NO}_3^-$ -N ion concentration reached 1.0 mg/L or less. The first to fourth adsorbent regeneration solutions used 1.0-M NaCl, whereas the fifth and sixth solutions employed 1.0-M HCl.

Fig. 7 depicts the breakthrough curve (data points) of  $\text{NO}_3^-$ -N ions as a function of the number of adsorbent uses, along with the theoretically calculated breakthrough curve (line) obtained by applying a numerical model formula. The  $\text{NO}_3^-$ -N breakthrough time and the stoichiometric time ( $C/C_0 = 0.5$ ) were shortened with an increasing number of uses when NaCl solution was used as the regeneration solution. However, considering that this shortening disappeared when HCl solution was used as a regeneration solution, it is thought to be caused by incomplete regeneration of the fixed-bed. Table 1 presents the characteristic constants calculated using the Bohart–Adams model as a numerical model equation for interpreting the breakthrough curve through linear regression analysis [21]. Regardless of the number of adsorbent uses, the calculated characteristic constants aligned with the Bohart–Adams model equation [22]. The rate constant  $K_{BA}$  increased within the error range until the third regeneration using 1.0-M NaCl, but it decreased from the fifth regeneration using 1.0-M HCl. When 1.0-M

NaCl was used as a regeneration solution, there was a clear tendency for the adsorption capacity  $N_0$  to decrease as the number of regeneration cycles increased. However, after washing the fixed-bed with 1.0-M HCl, its adsorption capacity recovered to a level similar to its initial use.

Fig. 8a illustrates the change in the  $\text{NO}_3^-$ -N concentration and regeneration efficiency as functions of the effluent waste liquid volume during the regeneration process. Within the fixed-bed column regeneration process, the effluent waste liquid exhibited a maximum peak  $\text{NO}_3^-$ -N concentration when the volume of the NaCl washing solution reached 7–8 times the fixed-bed. Subsequently, it rapidly decreased to less than 1.0 mg/L, 15–20 times the fixed-bed volume. The regeneration efficiency of the fixed-bed column was influenced by the regeneration solution type, resulting in a  $\text{NO}_3^-$ -N ion concentration of 3,500 mg/L when employing 1.0-M NaCl as the regeneration solution and an increase to 5,300 mg/L when using 1.0-M HCl (Fig. 8b).

#### 4. Conclusions

In this study, the efficiency of PAN-EDA nanofibers for nitrate–nitrogen ( $\text{NO}_3^-$ -N) removal from water was investigated. The synthesized PAN-EDA nanofibers demonstrated effective adsorption capabilities with an optimal adsorption capacity of 48 mg/g achieved at high EDA concentrations

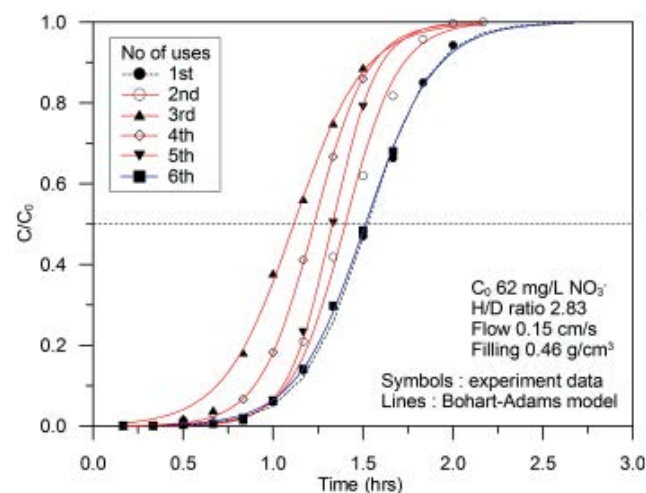


Fig. 7. Experimental and theoretical breakthrough curves for  $\text{NO}_3^-$ -N removal based on the number of repeated uses of polyacrylonitrile-ethylenediamine nanofiber adsorbent.

Table 1  
Parameters calculated from Bohart–Adams model

Operation cycle	$K_{BA}$ (L/mg·h)	$N_0$ (mg/L)	$q_0$ (mg/g)	$R^2$
1	0.0902	39,456	85.22	0.9915
2	0.1083	36,287	78.37	0.9948
3	0.1280	34,453	74.41	0.9983
4	0.1071	31,775	68.63	0.9998
5	0.0825	28,885	62.39	0.9966
6	0.0838	38,898	84.01	0.9986

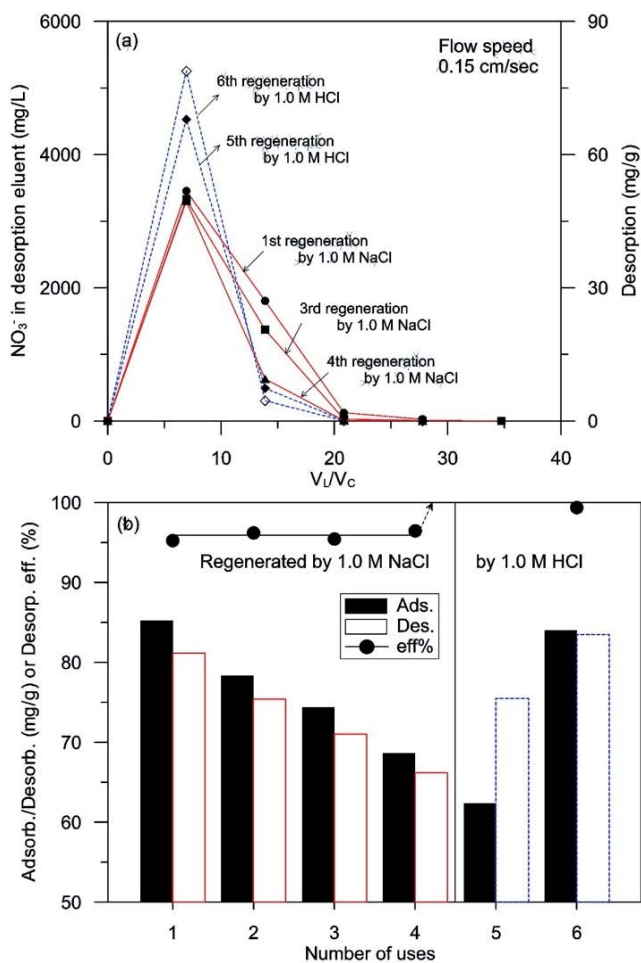


Fig. 8. Regeneration properties of polyacrylonitrile-ethylenediamine nanofibers using a solution of 1.0-M HCl and 1.0-M NaCl (a) in a fixed-bed column, and (b) based on the number of regenerations.

and elevated reaction temperatures. However, the capacity decreased owing to factors such as steric hindrance and saturation of adsorption sites over time, with the highest sustained adsorption capacity of 45 mg/g observed at 50% EDA concentration after 15 h.

The study also revealed the impact of the amination reaction temperature on the adsorption capacity of the PAN-EDA nanofibers. A higher adsorption capacity was observed at higher reaction temperatures owing to increased functionalization. However, higher temperatures were also linked to the degradation of the adsorption sites over time.

The physical and chemical properties of the PAN-EDA nanofibers, as assessed using SEM and FTIR analyses, revealed negligible changes in the nanofiber diameter after EDA modification but significant changes in their chemical composition. These chemical changes were largely attributed to the functionalization process with EDA, which introduced new functional groups, leading to more active adsorption sites for nitrate ions.

This study also confirmed that the pH of the solution significantly influences the adsorption efficiency. The

maximum adsorption rate of NO<sub>3</sub><sup>-</sup>-N by the PAN-EDA nanofiber was observed under weakly acidic conditions (pH 3–6), owing to the optimal electrostatic interactions between the nanofiber surface and NO<sub>3</sub><sup>-</sup>-N ions.

Fixed-bed column-based adsorption–regeneration experiments validated the promising potential of PAN-EDA nanofibers for practical applications, as the adsorbent demonstrated high regeneration efficiency, particularly when 1.0-M HCl was used as the regeneration solvent. The adsorbent's performance was sustained over several cycles of use, confirming its durability and reusability.

In conclusion, the PAN-EDA nanofibers provide a potentially effective and environmentally friendly solution for nitrate removal from water. These findings have important implications for wastewater treatment and environmental protection strategies, particularly in regions facing nitrate contamination challenges. Further studies would be beneficial for exploring the optimal synthesis and treatment conditions, gaining mechanistic insights, and scaling up the process for real-world applications.

#### Acknowledgements

This research was supported by a grant (RS-2022-00143411) from Regional Innovation Technology Development Program funded by Ministry of Land, Infrastructure and Transport of Korean government. This research was supported by the National Research Foundation of Korea (NRF-2020R111A1A01070853).

#### Data availability statement

All relevant data are included in the paper or its Supplementary Information.

#### References

- [1] J.N. Galloway, W. Winiwarter, A. Leip, A.M. Leach, A. Bleeker, J.W. Erisman, Nitrogen footprints: past, present and future, *Environ. Res. Lett.*, 9 (2014) 115003, doi: 10.1088/1748-9326/9/11/115003.
- [2] B. Singh, E. Craswell, Fertilizers and nitrate pollution of surface and ground water: an increasingly pervasive global problem, *SN Appl. Sci.*, 3 (2021) 518–542, doi: 10.1007/s42452-021-04521-8.
- [3] B. Bishayee, R.P. Chatterjee, B. Ruj, S. Chakraborty, J. Nayak, Strategic management of nitrate pollution from contaminated water using viable adsorbents: an economic assessment-based review with possible policy suggestions, *J. Environ. Manage.*, 303 (2022) 114081, doi: 10.1016/j.jenvman.2021.114081.
- [4] Z. Li, W. Xie, F. Yao, A. Du, Q. Wang, Z. Guo, H. Gu, Comprehensive electrocatalytic degradation of tetracycline in wastewater by electrospun perovskite manganite nanoparticles supported on carbon nanofibers, *Adv. Compos. Hybrid Mater.*, 5 (2022) 2092–2105, doi: 10.1007/s42114-022-00550-y.
- [5] P.L. Meena, K. Poswal, A.K. Surela, J.K. Saini, Synthesis of graphitic carbon nitride/zinc oxide (g-C<sub>3</sub>N<sub>4</sub>/ZnO) hybrid nanostructures and investigation of the effect of ZnO on the photodegradation activity of g-C<sub>3</sub>N<sub>4</sub> against the Brilliant Cresyl Blue (BCB) dye under visible light irradiation, *Adv. Compos. Hybrid Mater.*, 6 (2023) 16, doi: 10.1007/s42114-022-00577-1.
- [6] J. Yuan, Y. Amano, M. Machida, Surface modified mechanism of activated carbon fibers by thermal chemical vapor deposition and nitrate adsorption characteristics in aqueous solution, *Water Res.*, 580 (2019) 123710, doi: 10.1016/j.colsurfa.2019.123710.

- [7] T.F. Beltrame, D. Carvalho, L. Marder, M.A. Ulla, F.A. Marchesini, A.M. Bernardes, Comparison of different electrode materials for the nitrate electrocatalytic reduction in a dual-chamber cell, *Water Res.*, 8 (2020) 104210, doi: 10.1016/j.jece.2020.104120.
- [8] Z.B. Mokhtari-Hosseini, G.R. Bikhbar, T.S. Zare, Nitrate removal from aqueous solution: Screening of variables and optimization, *Adv. Environ. Technol.*, 1 (2023) 73–83, doi: 10.22104/AET.2023.5653.1596.
- [9] D.M. Martin, M. Faccini, M.A. García, D. Amantia, Highly efficient removal of heavy metal ions from polluted water using ion-selective polyacrylonitrile nanofibers, *J. Environ. Chem. Eng.*, 6 (2018) 236–245, doi: 10.1016/j.jece.2017.11.073.
- [10] J. Du, H. Xiong, Z. Dong, X. Yang, L. Zhao, J. Yang, Ethylenediamine and pentaethylene hexamine modified bamboo sawdust by radiation grafting and their adsorption behavior for phosphate, *Appl. Sci.*, 11 (2021) 7854–7868, doi: 10.3390/app11177854.
- [11] H. Dong, C.S. Shepsko, M. German, A.K. Sen Gupta, Hybrid nitrate selective resin (NSR-NanoZr) for simultaneous selective removal of nitrate and phosphate (or fluoride) from impaired water sources, *Water Res.*, 8 (2020) 103846, doi: 10.1016/j.jece.2020.103846.
- [12] M. Amarine, B. Lekhlif, E.M. Mlaji, J. Echaabi, Nitrate removal from groundwater in Casablanca region (Morocco) by electrocoagulation, *Groundwater Sustainable Dev.*, 11 (2020) 100452, doi: 10.1016/j.gsd.2020.100452.
- [13] R.S. Jasna, R. Gandhimathi, A. Lavanya, S.T. Ramesh, An integrated electrochemical-adsorption system for removal of nitrate from water, *J. Environ. Chem. Eng.*, 8 (2020) 104387, doi: 10.1016/j.jece.2020.104387.
- [14] S. Yang, C. Shi, K. Qu, Z. Sun, H. Li, B. Xu, Z. Huang, Z. Guo, Electrostatic self-assembly cellulose nanofibers/MXene/nickel chains for highly stable and efficient seawater evaporation and purification, *Carbon Lett.*, 33 (2023) 2063–2074, doi: 10.1007/s42823-023-00540-0.
- [15] F. Zhang, M. Lian, A. Alhadhrami, M. Huang, B. Li, G.A.M. Mersal, M.M. Ibrahim, M. Xu, Laccase immobilized on functionalized cellulose nanofiber/alginate composite hydrogel for efficient bisphenol A degradation from polluted water, *Adv. Compos. Hybrid Mater.*, 5 (2022) 1852–1864, doi: 10.1007/s42114-022-00476-5.
- [16] H. Zhou, Y. Tan, W. Gao, Y. Zhang, Y. Yang, Selective nitrate removal from aqueous solutions by a hydrotalcite-like absorbent FeMgMn-LDH, *Sci. Rep.*, 10, (2020) 16126–16136, doi: 10.1038/s41598-020-72845-3.
- [17] M.M. Sabzehmeidani, M. Ghaedi, Chapter 5 – Adsorbents Based on Nanofibers, *Interface Science and Technology*, 33 (2021) 389–443, doi: 10.1016/B978-0-12-818805-7.00005-9.
- [18] A. Gul, N.G. Khaligh, N.M. Julkapli, Surface modification of carbon-based nanoadsorbents for the advanced wastewater treatment, *J. Mol. Struct.*, 1235 (2021) 130148, doi: 10.1016/j.molstruc.2021.130148.
- [19] B.R. Broujeni, A. Nilchi, Preparation and characterization of polyacrylonitrile nanofiber adsorbent modified with 6-amino-1-hexanethiol hydrochloride for the adsorption of thorium(IV) ion from aqueous solution, *Desal. Water Treat.*, 133 (2018) 122–133, doi: 10.5004/dwt.2018.23001.
- [20] Q. Hu, H. Liu, Z. Zhang, Y. Xie, Nitrate removal from aqueous solution using polyaniline modified activated carbon: optimization and characterization, *Water Res.*, 309 (2020) 113057, doi: 10.1016/j.molliq.2020.113057.
- [21] Z. Jamka, W. Mohammed, Assessment of the feasibility of modified chitosan beads for the adsorption of nitrate from an aqueous solution, *J. Ecol. Eng.*, 24 (2023) 265–278, doi: 10.12911/22998993/156886.
- [22] G.S. Bohart, E.Q. Adams, Some aspects of the behavior of charcoal with respect to chlorine, *J. Am. Chem. Soc.*, 42 (1920) 523–544, <https://doi.org/10.1021/ja01448a018>.